

Design, Simulation, and Fabrication of Piezoelectric based detection of Doctor's Hand Tremor



By

Abdullah Qamar

(Registration No 00000328036)

Supervised by

Dr. Muhammad Osama Ali

Department of Mechatronics Engineering

College of Electrical & Mechanical Engineering

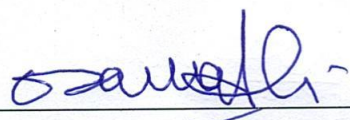
National University of Sciences & Technology (NUST)

Islamabad, Pakistan

(Aug 2024)

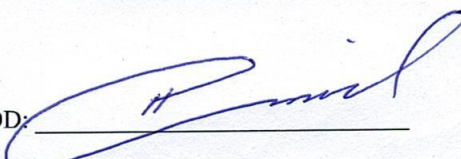
THESIS ACCEPTANCE CERTIFICATE

Certified that final copy of MS/MPhil thesis by Mr. Abdullah Qamar Registration No. 328036, of Electrical and Mechanical Engineering College has been vetted by undersigned, found complete in all respects as per NUST Statues/Regulations, is free of plagiarism, errors, and mistakes and is accepted as partial fulfillment for award of MS/MPhil degree. It is further certified that necessary amendments as pointed out by GEC members of the scholar have also been incorporated in the said thesis.

Signature: 

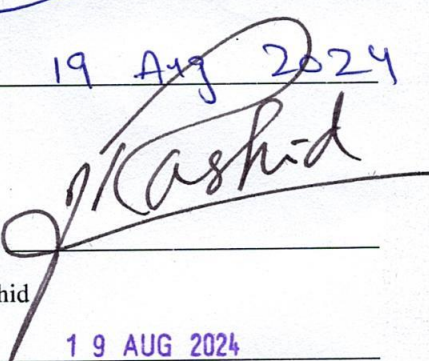
Name of Supervisor: Dr. Muhammad Osama Ali

Dated: 19 Aug 2024

Signature of HOD: 

Dr. Hamid Jabbar

Date: 19 Aug 2024

Signature of Dean: 

Brig Dr. Nasir Rashid

Date: 19 AUG 2024

DEDICATION

I want like to dedicate this work to my parents and siblings, whose support and sacrifices have been my greatest motivation.

ACKNOWLEDGEMENTS

I extend my deepest gratitude to my supervisor Dr. Muhammad Osama Ali for his exceptional insight and scholarly guidance throughout the process of completing my thesis. His expertise, dedication, and unwavering support have been instrumental in shaping both the direction of my research and my personal growth as a scholar.

I am also thankful to Dr Hassan Elahi for his understanding, core expertise, and constructive criticism, which proved crucial in navigating this research endeavor.

I am equally grateful to my Guidance and Evaluation Committee Members Dr. Mohsin Islam Tiwana and Dr Anas Bin Aqeel for their continuous feedback, encouragement, and guidelines, which motivated and propelled me forward.

ABSTRACT

In this study, we present a new vibration energy harvester that aims to harness the involuntary hand movements associated with vibration. The device features a special single-beam design with a piezoelectric component located at the principal point. We used both experimental and computational methods to analyze the performance of the harvester in the study. In practical tests, a rather low resonant frequency of 7.5 Hz emerged, which is consistent with the 8.0373 Hz predicted by the Finite Element Method (FEM) simulation. Variations in material properties and manufacturing tolerances result in these small variations. A mass-spring mechanism combined with a cantilever beam concept forms the basis of the combined design. This arrangement increases the bending moment of the beam, maximizing the energy conversion efficiency. The results of experimental evaluation in an open-loop environment were encouraging. At a resonant frequency of 7.5Hz, the device generated an impressive peak-to-peak voltage of 11.44V. When connected to an ideal load resistance of 470k Ω , the maximum output power of the combine was 63.89 μ W. These results show how our system can be used to harvest energy from low-frequency vibrations, especially those caused by physical impact. The combine's ability to generate large amounts of energy with small hand movements indicates potential applications in medical and wearable technology.

Keywords: Energy Harvester, Hand Tremor, Single Degree of Freedom (SDOF), Wearable technology, Piezoelectric, Tremor, Parkinson's disease, Eye surgery, Hand Glove.

CONTENTS

ACKNOWLEDGEMENTS	IV
ABSTRACT	V
LIST OF TABLES	VII
LIST OF FIGURES	VIII
CHAPTER 1: INTRODUCTION	1
1.1 Problem Formulation	3
1.2 Research Objectives	4
CHAPTER 2: LITERATURE REVIEW	5
CHAPTER 3: METHODOLOGY	15
3.1 Shape optimization	16
3.2 Final Form	18
3.3 Holding Mechanism	19
CHAPTER 4: FINITE ELEMENT METHOD	23
CHAPTER 5: EXPERIMENTAL SETUP	25
5.1 Results and Discussion	28
CHAPTER 6: CONCLUSION	35

LIST OF TABLES

	Page No.
Table 3.1.1: Structural properties of the Beam of Energy Harvester	17
Table 3.1.2: Structural properties of the Proof Mass of Energy Harvester	18
Table 4.0.1: Material used and their properties.....	24

LIST OF FIGURES

	Page No.
Figure 2.0.1: Proposed Piezoelectric Energy Harvester [18].....	5
Figure 2.0.2: Proposed Piezoelectric Energy Harvester [19].....	6
Figure 2.0.3: Proposed Piezoelectric Energy Harvester [20].....	6
Figure 2.0.4: Proposed Piezoelectric Energy Harvester [21].....	7
Figure 2.0.5: Proposed Piezoelectric Energy Harvester [22].....	7
Figure 2.0.6: Proposed Energy Harvester [23]	8
Figure 2.0.7: Proposed Piezoelectric Energy Harvester [24].....	8
Figure 2.0.8: Proposed Energy Harvester [25]	9
Figure 2.0.9: Proposed Energy Harvester [26]	10
Figure 2.0.10: Proposed Piezoelectric Energy Harvester [27].....	10
Figure 2.0.11: Proposed Piezoelectric Energy Harvester [28].....	11
Figure 2.0.12: Proposed Energy Harvester [29]	11
Figure 2.0.13: Proposed Energy Harvester [30]	12
Figure 2.0.14: Proposed Energy Harvester [31]	12
Figure 2.0.15: Proposed Energy Harvester [32]	13
Figure 2.0.16: Proposed Energy Harvester [33]	13
Figure 2.0.17: Proposed Energy Harvester [34]	13
Figure 2.0.18: Proposed Energy Harvester [35]	14
Figure 2.0.19: Proposed Energy Harvester [36]	14
Figure 3.1.1: Final Schematic of the Proposed Energy Harvester	16
Figure 3.1.2: Other shapes for the Analysis (a) with square multiple masses	16
Figure 3.1.2: Other shapes for the Analysis (b) with circle multiple masses	17
Figure 3.2.1: Final dimensions of the beam of the Energy Harvester	18
Figure 3.2.2: Final dimensions of Proof Mass of the Energy Harvester.....	19
Figure 3.3.1: Energy Harvester assembled on the holding assembly	20
Figure 3.3.2: Prototyped Energy Harvester assembled on the holding assembly	21
Figure 3.3.3: Prototyped Energy Harvester held on the hand through strip	22
Figure 4.0.1: Harmonic Frequency of the proposed model at first resonant frequency (8.0373 Hz)	23
Figure 4.0.2: Harmonic Frequency of the proposed model at second resonant frequency (22.689 Hz)	24
Figure 5.0.1: Photograph of the Function Generator	25
Figure 5.0.2: Photograph of the Vibration Exciter	26
Figure 5.0.3: Photograph of the Power Amplifier	26
Figure 5.0.4: Photograph of the Digital Oscilloscope.....	26
Figure 5.0.5: Photograph of the Experimental setup with fabricated proposed Energy Harvester prototype.....	27
Figure 5.1.1: Frequency response of the proposed energy harvester.....	29
Figure 5.1.2: Output power vs Load resistor of the piezoelectric beam of the proposed energy harvester at 7.4 Hz.....	30

Figure 5.1.3: Output power vs Load resistor of the piezoelectric beam of the proposed energy harvester at 7.5 Hz.....	31
Figure 5.1.4: Output power vs Load resistor of the piezoelectric beam of the proposed energy harvester at 7.6 Hz.....	31
Figure 5.1.5: Instantaneous voltage waveform generated by the single piezo element of the proposed energy harvester prototype at 7.4 Hz.....	32
Figure 5.1.6: Instantaneous voltage waveform generated by the single piezo element of the proposed energy harvester prototype at 7.5 Hz.....	32
Figure 5.1.7: Instantaneous voltage waveform generated by the single piezo element of the proposed energy harvester prototype at 7.6 Hz.....	33

CHAPTER 1: INTRODUCTION

In recent years, advances in remote control technology have significantly improved the performance of robots. These advanced robots are now being used in various industries, including space exploration and medicine[1]. Various instabilities such as operator handshake and communication delays affect remote operation systems. In remote operation, this shock, which is a natural physical phenomenon, can make it difficult to perform tasks accurately[1][2][3].

Cardiovascular diseases are one of the leading causes of morbidity and mortality in modern medicine. People affected by such diseases often experience pain and disability. More and more physicians are using minimally invasive surgery to treat these high-risk cardiovascular diseases. Vascular interventional surgery (VIS) is one popular strategy, offering a less invasive alternative to open surgical techniques to treat various cardiac diseases[4]. When Kwoh performed a neurosurgical needle biopsy under CT guidance using a PUMA 560 robotic surgical arm in 1985, it marked the first time robot-assisted surgery was documented in a human patient. Robotic surgery has become a rapidly expanding field of medicine, contributing to advances in surgical care and potentially becoming widely used in many surgical specialties. Robotic systems currently under development promise improvements in scope, efficiency, effectiveness, reproducibility, safety, and cost compared to manually performed surgery. Their heightened accuracy, capacity for repeatable performance, and ability to get around some physiological constraints unique to humans are some of the reasons for this. The required ability of human-robot interaction is further extended by integrating robotics with other support capabilities like image systems and sensors[5].

Tremors are unintentional, uncontrollable, irregular contractions of muscles that cause one or more bodily parts to shake. Depending on the medical and physical condition, tremors may vary in magnitude, frequency, and duration. Tremors can be categorized based on their appearance, cause, or origin. They can also be intermittent or persistent, occur on their own, or as a result of an underlying medical condition[6]. Tremors are irregular,

involuntary movements of any part of the body. These uncontrollable movements might seriously impede activities linked to work and personal life. Although maintaining body posture is a usually efficient function of the human motor system, it is an intrinsically difficult function. The complexity results from the large number of factors that go into bodily alignment and the complex nervous system controls that are needed. Because of this, even slight perturbations to this system can cause audible tremors, emphasizing the fine balance needed for efficient motor control[7]. The tremor that naturally occurs in a surgeon's hands is one of the biggest obstacles when completing treatments for retinal membrane removal. The inability to control this movement can present serious challenges to carrying out the procedure correctly. More importantly, it significantly raises the risk that surgical equipment will unintentionally come into touch with sensitive eye tissues, potentially injuring the retina. Such iatrogenic injuries may arise during this extremely precise technique if the surgeon's hand tremors produce uncontrollable movements of the surgical instruments[5].

Among neurological conditions that cause movement problems, Essential Tremor (ET) is particularly common. It is widely recognized for its frequent occurrence and the significant effects it can have on those who are impacted. Individuals who are diagnosed with ET frequently face significant obstacles in their physical abilities as well as in their social relationships, which may result in significant impairments to their overall quality of life [8].

Physiological hand tremor is a well-identified component of unwanted and uncontrollable hand movement. The hand oscillates uncontrollably, usually with an amplitude of 50 to 200 micrometers, as a result of this condition. These tremors often have frequencies between 6 and 12 Hz, and they have a quasi-rhythmic, sinusoidal pattern[7].

Every part of the human body experiences vibrations along each major axis, typically on the scale of 50-100 micrometers. The frequency range of 8-12 Hz is where most of these vibrations occur[1][9][10].

These tremors are a constant in both dynamic hand movements and static hand postures. When it comes to microsurgical treatments, these tremors are quite dangerous. The delicate tissues being operated on may be harmed by the minute, erratic motions. Understanding

this risk, microsurgeons use a variety of methods and approaches to reduce the impact of their innate hand tremors during sensitive procedures[7].

There are several ways to convert mechanical vibrations into electrical energy, but three main mechanisms stand out. One of the main strategies is the piezoelectric effect. Electrostatic and electromagnetic transport are among the three known ways to obtain energy from mechanical motion[11][12][13][14][15]. Piezoelectric transducers are particularly good at converting mechanical energy into electrical energy, making them stand out among other energy conversion technologies. Their dominance is the result of their unusually high energy density of 35.4mJ/cm^3 . This incredible density allows piezoelectric-based vibration energy harvesters to achieve unprecedented efficiencies. Such devices are capable of generating much more energy than other types of transducers of similar size, making them an excellent choice for many energy-harvesting applications[16].

PZT (Lead Zirconate Titanate) is a lead-based polycrystalline ceramic that has become the most popular piezoelectric material in the field of vibration energy harvesting. PZT's formula, $\text{Pb} [\text{Zr}_x\text{Ti}_{1-x}] \text{O}_3$, is a malleable material with modifiable properties. PZT is widely used due to several key advantages. Chief among them is that it can be easily adapted to mass production techniques, significantly reducing manufacturing costs. The low cost makes PZT a desirable choice for commercial applications. Not only that, but PZT offers incredible manufacturing flexibility. Engineers can mold and shape the material to meet a variety of parameters, customizing the material's shape to meet the specific requirements of different applications and energy harvesting devices[17]. Using piezoelectric materials for vibration energy harvesters at low frequencies is always challenging and requires creative structural design[18].

1.1 Problem Formulation

Anyone can experience tremors, especially if they hold their hands for a long time. These behaviors are very annoying when in an operating situation the surgeon needs to maintain the correct position of the hand for several hours. In the course of such treatment, patients

can face considerable risks if they receive unwanted shocks. While these small movements are often unnoticeable in everyday life, they can have a significant impact on high-precision work. Not only can it be difficult for surgeons to regulate their physical tremors, but it can also be difficult for surgical outcomes to minimize the effects of tremors. New technologies are being developed to solve this problem, such as de-tremors and robotic-assisted surgery. Research is also ongoing to identify the root cause of such tremors and develop non-invasive strategies to reduce them. This research could significantly improve patient safety and surgical precision.

1.2 Research Objectives

- Design a mesoscale piezoelectric-based Energy Harvester for the detection of Doctor's hand tremor.
- Analysis of the mesoscale piezoelectric-based Energy Harvester for the detection of a Doctor's hand tremor.
- Fabrication and Testing of the mesoscale piezoelectric-based Energy Harvester.
- Validation of the Numerical and Experimental Model of the Energy Harvester.

CHAPTER 2: LITERATURE REVIEW

In 2017 R.M. Toyabur et al. proposed and experimentally validated a piezoelectric multimodal energy harvester with multiple degrees of freedom, designed to operate efficiently at lower ambient vibration frequencies. The unique design allows for multiple resonant modes in the 10-20 Hz range, with peak values around 10, 14, 16, and 20 Hz, as predicted by finite element method simulations and confirmed by experimental results. The prototype uses lead zirconate titanate (PZT) as the piezoelectric material and incorporates four piezoelectric elements. When connected in parallel, these elements generate a peak output power of $740 \mu\text{W}$ at the third resonant mode (16 Hz) under 0.4 g base acceleration, demonstrating improved performance over conventional single-degree-of-freedom systems[18].

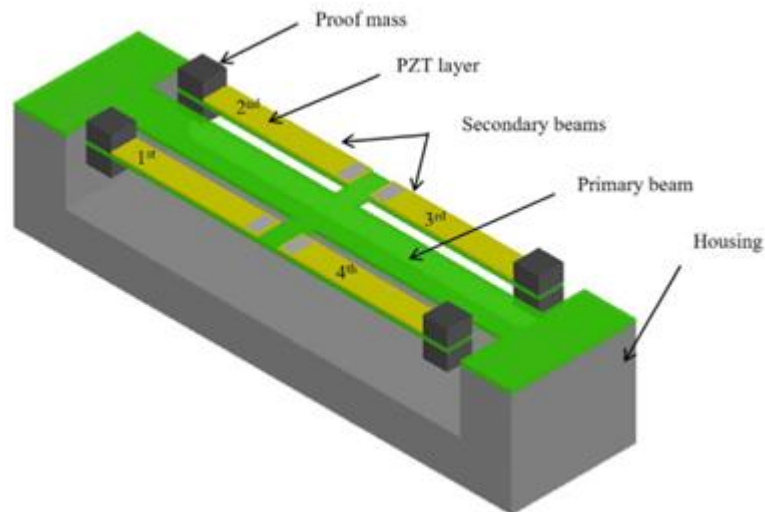


Fig 2.0.1 – Proposed Piezoelectric Energy Harvester [18]

J.M. Ramirez et al. present a novel low-frequency vibration-based energy harvester (VEH) for powering wireless monitoring systems in 30kW wind turbines. The device is designed to operate in the 3-10 Hz range, using multi-beam cantilevers with tip masses to enhance its bandwidth. Of the four designs evaluated, the most effective configuration uses two multiple-beam tridents joined by a rigid beam. This design produces up to $96.04 \mu\text{W}$

at its second resonance frequency, exceeding the $20 \mu\text{W}$ required for autonomous wireless monitoring applications[19].

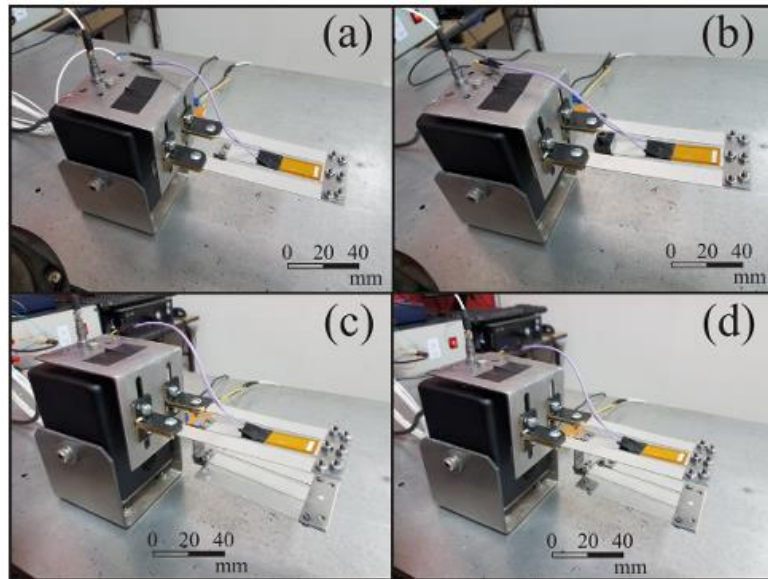


Fig 2.0.2 – Proposed Piezoelectric Energy Harvester [19]

In 2022, Jiansu Wang et al. reported work on a vibration energy harvester with frequencies between 8 and 20 Hz, measuring $40 \times 41 \times 0.5 \text{ mm}$. The multilayer copper device had a voltage of up to 9.2 V and a maximum power of $29 \mu\text{W}$. To verify the functionality of a prototype created specifically for human motion applications, the researchers put it to real-world testing[20].

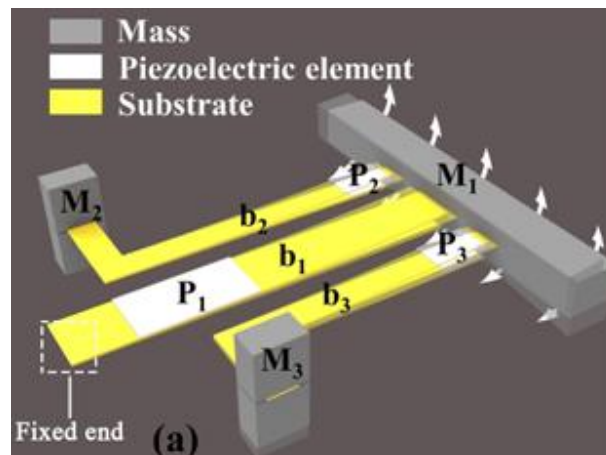


Fig 2.0.3 – Proposed Piezoelectric Energy Harvester [20]

David et al. present a unique low-frequency serpentine piezoelectric vibration energy harvester for sensor node applications. The device maintains a 1:1 aspect ratio while achieving a low resonant frequency, making it suitable for sensor nodes. The collector uses laser-machined PZT bimorphs with voltage-matched electrodes (SME) and voltage-matched polarization (SMP) techniques to minimize voltage cancellation issues. The prototype, measuring only 27×23 mm in size and 6.5 mm in height, generates $118 \mu\text{W}$ at 49.7 Hz when subjected to an acceleration of 0.2 g. This demonstrates the feasibility of efficiently harvesting energy from sub-100 Hz vibration sources in a small package[21].

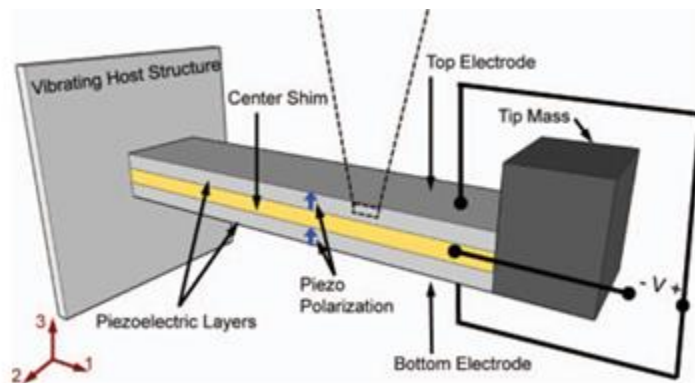


Fig 2.0.4 – Proposed Piezoelectric Energy Harvester [21]

In 2020, Siyang Hu et al. Presented a second multiplexed energy harvester. This device operates in the 66-80 Hz frequency band and is made of steel sheets. With a maximum output power of $1 \mu\text{W}$, it shows the potential for energy harvesting applications in high-frequency environments.[22].

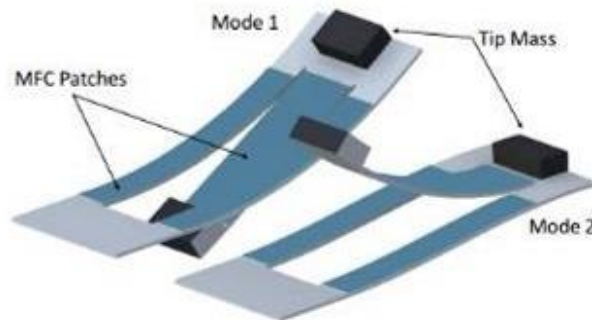


Fig 2.0.5 – Proposed Piezoelectric Energy Harvester [22]

This work aims to present a multi-mode vibration energy harvester that overcomes the shortcomings of existing cantilever harvesters, which are usually limited to a single performance frequency range. The proposed device, combined with a spiral cantilever and a magnetolectric (ME) transducer with a magnetic tip mass, exhibits a wide operating range and many peaks in the frequency response. As can be seen from the experimental results, magnetic coupling can reduce the distance between the variable peak frequency and adjacent modes, which shows that this design achieves five unique peak values between 15 and 70 Hz[23].

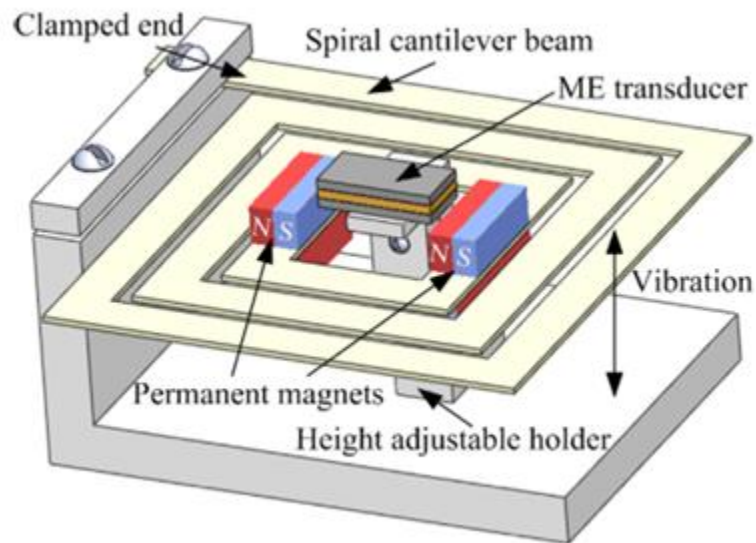


Fig 2.0.6 – Proposed Energy Harvester [23]

Chunkang Shi et al. introduced a foldable multi-layer energy harvester in 2020. With a maximum power of $336 \mu\text{W}$, this brass device is ideal for frequencies between 58 and 136 Hz. With dimensions of $26 \times 5 \times 90 \text{ mm}$ per screen, it is larger and more powerful than previous models. The design of this combination allows it to support much more weight than the above-mentioned equipment[24].

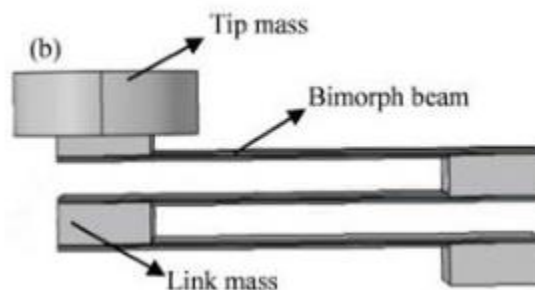


Fig 2.0.7 – Proposed Piezoelectric Energy Harvester [24]

In their work, Ando et al. presented a novel nonlinear broadband energy harvester. The basic operating principle of the device is nonlinearity due to mechanical loading, which is incorporated into the innovative design. The combine is compact and efficient with dimensions of 10 x 100 mm. The design is primarily made from the ubiquitous plastic polyethylene terephthalate (PET). Surprisingly, a plastic roller, easily available in most stationery stores, is used to illustrate the idea. The combined design also includes well-placed stop devices to increase efficiency[25].

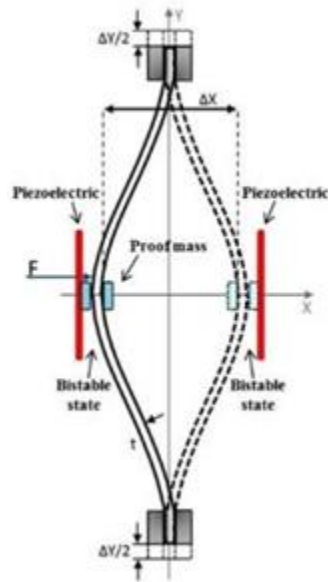


Fig 2.0.8 – Proposed Energy Harvester [25]

In their paper, Weile Jiang et al. described an energy harvester made from polymethyl methacrylate (PMMA). The device operates in two frequency ranges: 6-12 Hz in a U-shaped design and 7-22 Hz in an L-shaped design. The harvester measures 60 x 60 x 20 mm and can generate up to 0.4 μ W of power[26].

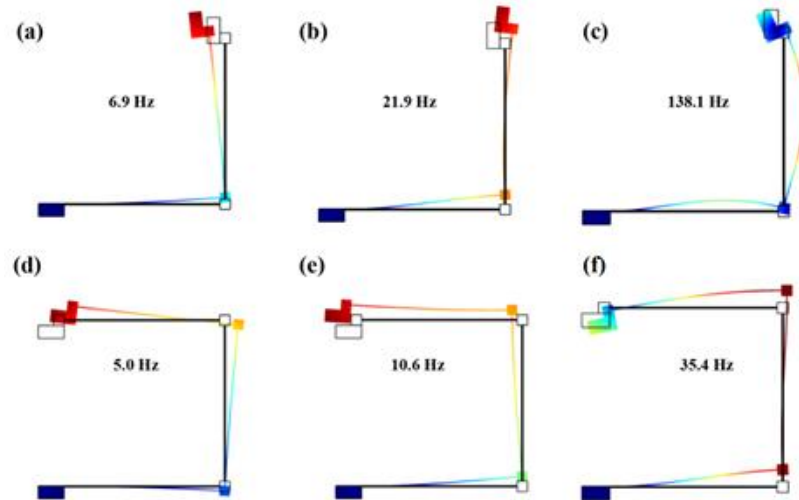


Fig 2.0.9 – Proposed Energy Harvester [26]

Zhao and his colleagues introduced an innovative energy harvester with a unique tubular circular spring geometry. Beryllium bronze was used in the construction of this device due to its unique mechanical properties. The combine is designed to work well between 16-28Hz depending on the frequency. When operating at maximum efficiency, the device delivers an astounding performance of up to $330\mu\text{W}$ [27].

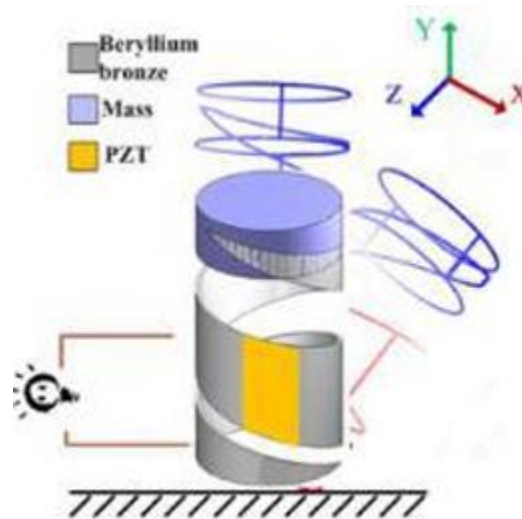


Fig 2.0.10 – Proposed Piezoelectric Energy Harvester [27]

Wu et al. presented an innovative energy-harvesting design in 2018. The device has a vertical bulldog clip and a hanging mass that resembles a pendulum. This combination generates an impressive 13.29 MW of power with a frequency conversion factor of 2 even in the low operating frequency range of 1 to 3.2 Hz. The low-frequency range is specifically designed to capture energy with the march of a walking human[28].

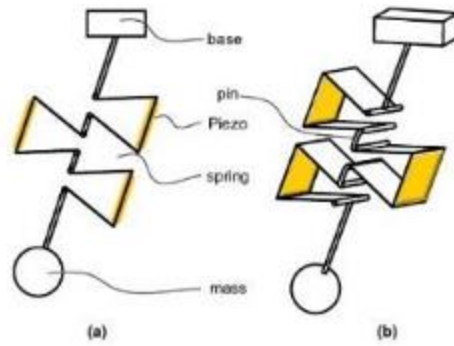


Fig 2.0.11 – Proposed Piezoelectric Energy Harvester [28]

Some designs in the field of nonlinear energy harvesting use the internal resonance principle to improve efficiency. A study published in a particular year (registered year) provides a notable example of this approach. Following the instructions (including the author's name), the researchers incorporated magnets into the combined design. These creative arrangements produced surprising results, greatly increasing the instrument's electrical output. They also significantly increased the operating frequency range of the combine, allowing it to operate successfully over a wide frequency range from 71Hz to 143Hz[29].

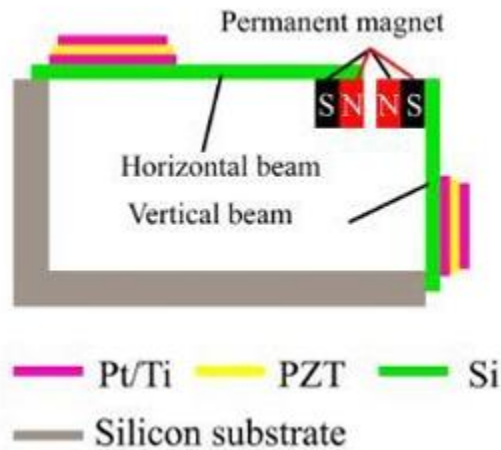


Fig 2.0.12 – Proposed Energy Harvester [29]

A 2019 study by Yuan et al. looked at the use of a plug-in energy harvester. The stainless steel device measures 20 x 110 x 9.5 mm. The bond produces 8.3 MW of power and works well in the 20-50 Hz frequency range[30].

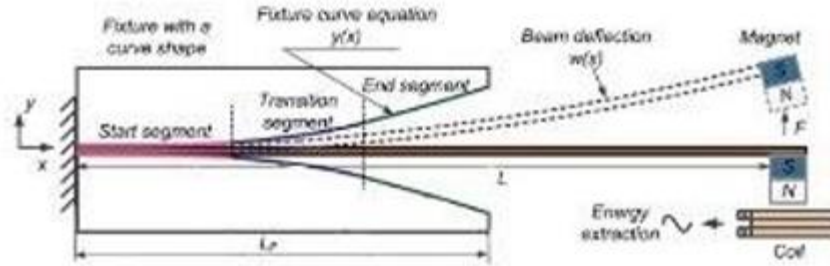


Fig 2.0.13 – Proposed Energy Harvester [30]

In 2019, Ushiki and colleagues described an energy harvester utilizing neodymium magnets. This device operates within a frequency range of 35 to 70 Hz and can generate up to 1.8 mW of output power[31].

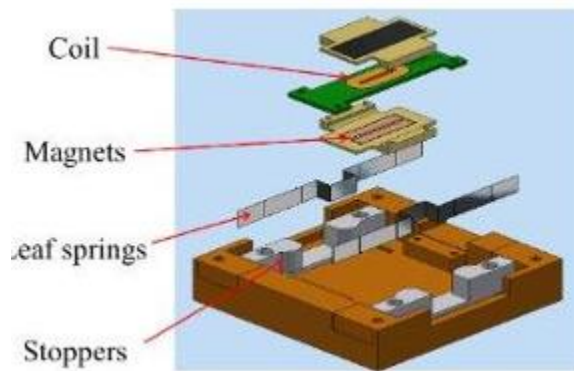


Fig 2.0.14 – Proposed Energy Harvester [31]

Dilpreet Bath et al. proposed a foldable multi-layer energy harvester using stainless steel in 2018. The device measures 30 x 31 x 6 mm and has an operating frequency range of 90-160 Hz. Both layers have multiple piezoelectric strips and can generate 1.8 MW of peak power[32].

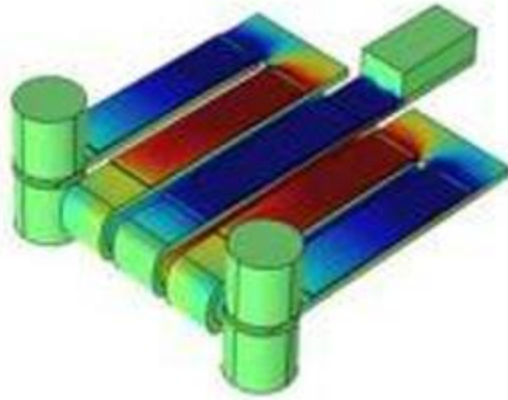


Fig 2.0.15 – Proposed Energy Harvester [32]

Han et al. have built a frequency-up converting harvester similar to the PET device described above: this compact harvester is 4×10 mm in size and operates at frequencies between 12 and 77 Hz, with a frequency-up conversion factor of 6.4 and a maximum power output of $7 \mu\text{W}$ [33].

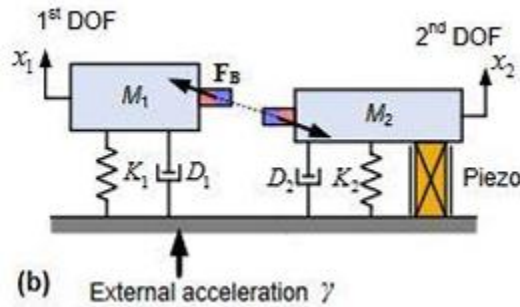


Fig 2.0.16 – Proposed Energy Harvester [33]

Masana et al. developed an aluminum-based energy harvester. This device measures $150\text{mm} \times 13\text{mm} \times 0.6\text{mm}$ and operates within a frequency range of 8 to 55 Hz[34].

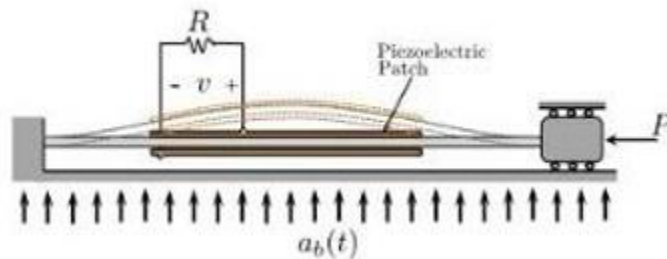


Fig 2.0.17 – Proposed Energy Harvester [34]

In a study by Lihua Tang et al., an energy harvester made of aluminum was created. With the cap included as the main design element, the device can generate up to $1.01\mu\text{W}$ of power. The size of the combine is 10mm wide, 0.6mm thick, and 70mm long. It is specifically designed to perform well in the frequency range of 23-30Hz[35].

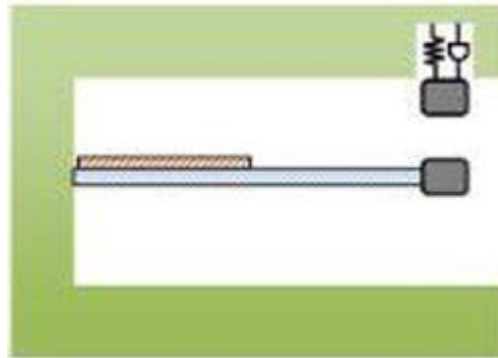


Fig 2.0.18 – Proposed Energy Harvester [35]

Tang et al. have developed a frequency-up-converting energy harvester tailored to ocean wave conditions. The aluminum device measures 10 x 100 mm and operates between 7 and 40 Hz, depending on the frequency. It is primarily designed for ocean wave energy harvesting and other similar induced displacement situations[36].

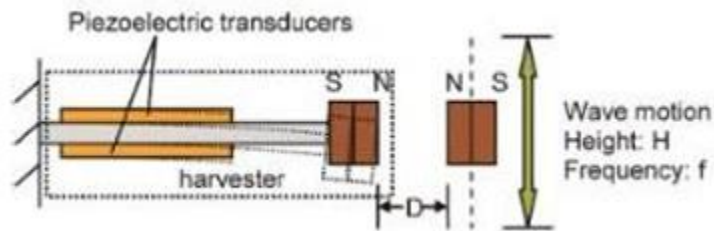


Fig 2.0.19 – Proposed Energy Harvester [36]

CHAPTER 3: METHODOLOGY

Conventional single-degree of-freedom (SDOF) energy harvesters convert mechanical vibrations into electrical energy through a direct arrangement of masses and springs. To record the bending moment of a beam, a piezoelectric element is usually used in the form of a cantilever beam with a test mass, connected to the system.

A cantilever beam, fixed at one end and free at the other, is the simplest type of energy harvester. This design is typically evaluated in a single degree of freedom, as it essentially operates at a single resonant frequency that is optimal for energy harvesting [37]. Taking this into account, the system can feed more beams to generate more spikes, which means that each beam has a unique resonant frequency depending on its material, shape, and dimensions. However, there is a limitation in our design that this Energy Harvester has to be worn at the doctor's Hand so it needs to be a single cantilever beam as multiple cantilever beams can be a hurdle to the doctor's hand during surgery.

The stressed area of the beam is another important consideration. The resulting stresses are always at the fixed end of the beam, as shown in Figure 3.0.1 below. Also, where you place the piezoelectric strips is important, as placing the elements on a low-voltage beam would be useless as they would not deform or leak.

In 2020, Nishanth et al. investigated the use of Aluminum Nitride (AlN) in MEMS technology for piezoelectric vibration energy harvesters (PVEHs), focusing on optimizing geometric parameters for low resonant frequency and high power output. According to the researchers, the best-performing beam was a trapezoidal beam with a triangular test mass

covering 57%-80% of the combine's length. When placed in an array, the improved design produces $0.24 \mu\text{W}$ at 158.8 Hz with an input acceleration of 0.5 G, generating 1.79 times more power at a low resonant frequency than a conventional rectangular combine[38].

3.1 Shape optimization

We have tried different shapes of beams with different shapes of masses to check the frequency response that closely fits our desired frequency range which is from 6 Hz to 10 Hz. After multiple analyses and simulations, we finalized this design.

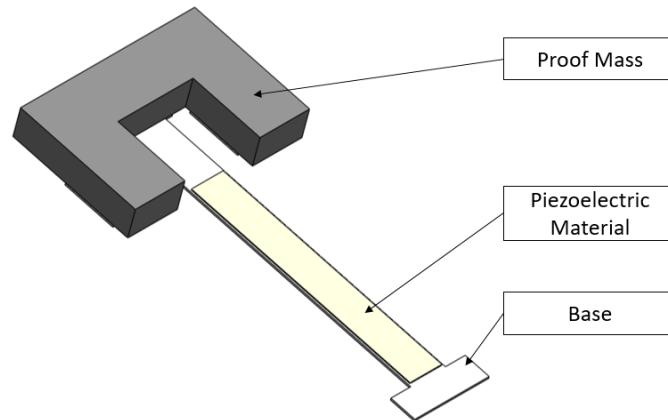
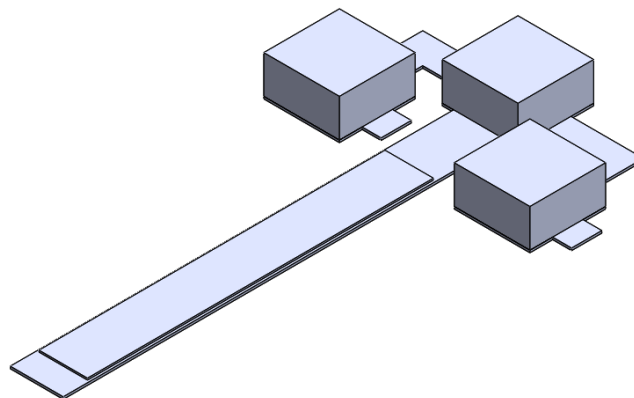
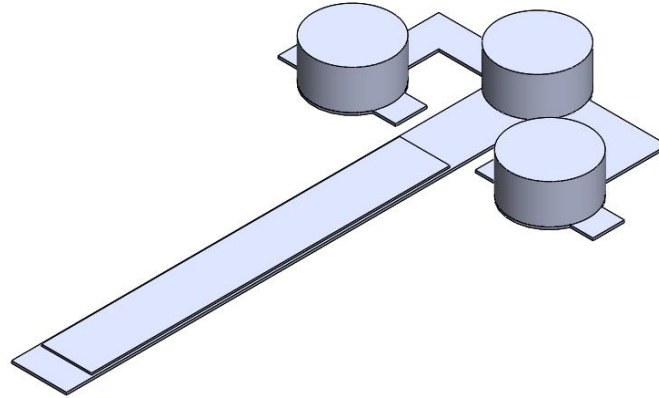


Figure 3.1.1 – Final Schematic of the Proposed Energy Harvester



(a)



(b)

Figure 3.1.2 – Other shapes for the Analysis (a) with square multiple masses (b) with circle multiple masses

Table 3.1.1: Structural Properties of the Beam of Energy Harvester

Length	68.5 mm
Width	7
Thickness	0.5
Material	Aluminum Density: 2780 kg/m ³ Young's Modulus: 70 GPa Poisson's Ratio: 0.33

Table 3.1.2: Structural Properties of the Proof Mass of Energy Harvester

Length	35 mm
Width	24
Thickness	6
Material	Aluminum Density: 7860 kg/m ³ Young's Modulus: 210 GPa Poisson's Ratio: 0.3

3.2 Final Form

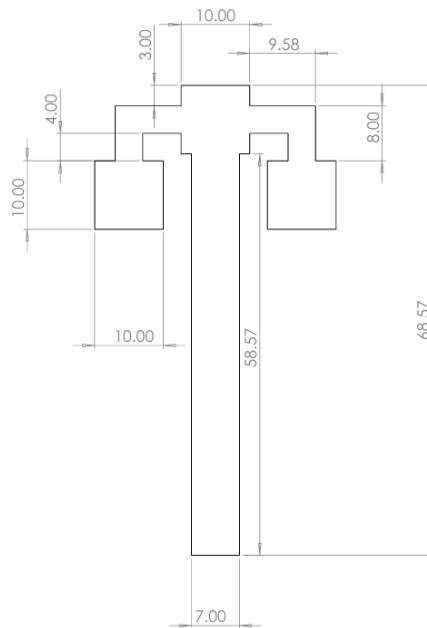


Figure 3.2.1 – Final dimensions of beam of the Energy Harvester

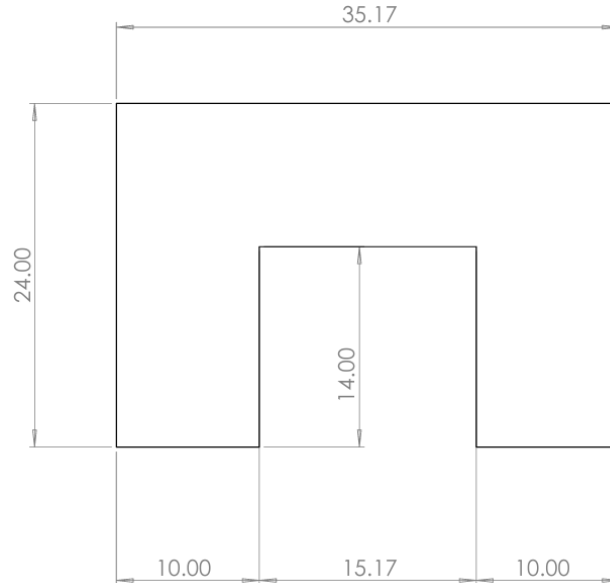


Figure 3.2.2 – Final dimensions of Proof mass of the Energy Harvester

Figure 3.2.1 shows the final form of the Beam of the Energy Harvester in mm. The harvester consists of a single beam where one end of the harvester is fixed and the proof mass is attached to the other end of the beam. The dimension of the Proof mass is shown in Figure 3.2.2.

3.3 Holding Mechanism

Our proposed design is engineered to fit comfortably on a doctor's hand and can be secured with a band. It features a single-clamped beam integrated with a piezoelectric (PZT) element for energy harvesting. When subjected to transverse vibrations, the flexible beam acts as a primary linear transmission component. This causes the beam to oscillate relative to the combined base when driven by external mechanical vibrations.

The single resonant frequency of this system is tuned to match viable ambient frequencies. In essence, the entire setup functions as an SDOF system. As the beam vibrates, it

experiences significant internal stresses, which in turn generate mechanical stresses on the surfaces of the piezoelectric element. These mechanical stresses are then converted into voltage and power output.

This design offers several advantages over traditional energy harvesting methods. By aligning the system's resonant frequency with common ambient vibrations, it can more efficiently capture energy from the environment. The compact nature of the device makes it particularly suitable for medical applications, where it can potentially harvest energy from a surgeon's hand movements without interfering with their work.

Moreover, the simplicity of the SDOF system enhances its reliability and ease of manufacture. The use of a piezoelectric element allows for the direct conversion of mechanical stress into electrical energy, eliminating the need for complex electromagnetic components. This not only reduces the overall size of the device but also potentially increases its durability and longevity in practical applications.

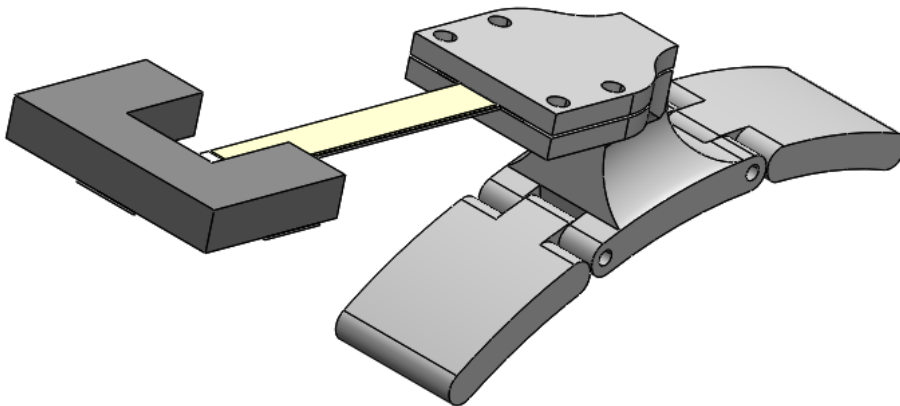


Figure 3.3.1 – Energy Harvester assembled on the holding assembly

Figure 3.3.1 shows the detailed assembly of the Harvester along with the holding mechanism of the Hand. While the prototype of the Harvester is shown in Figure 3.32 and

Figure 3.3.3. The prototype is made up of a primary beam made of Aluminum Material. This material has a low Young's modulus which helps to match the resonance of the energy harvester with the excitation of ambient vibrations. Laser technology is used to cut down the beam in the same dimensions. PZT ceramic material (5 A Navy Type II) is used to harvest the energy that can be used to detect the tremor in the doctor's hand by Piezo Systems, Inc. A specific procedure has been used to manufacture the piezoelectric material used in this study. First, the PZT (Lead Zirconate Titanate) surface was treated with nickel electrodes by vacuum sputtering. The material was then poled, applying an electric field throughout the thickness of the material. The producer supplied us with raw PZT in the form of large ceramic sheets. We carefully cut the sheets with a high-precision saw equipped with a diamond blade to obtain the size and shape required for the experiments. After that PZT is attached to the beam by using epoxy adhesive.

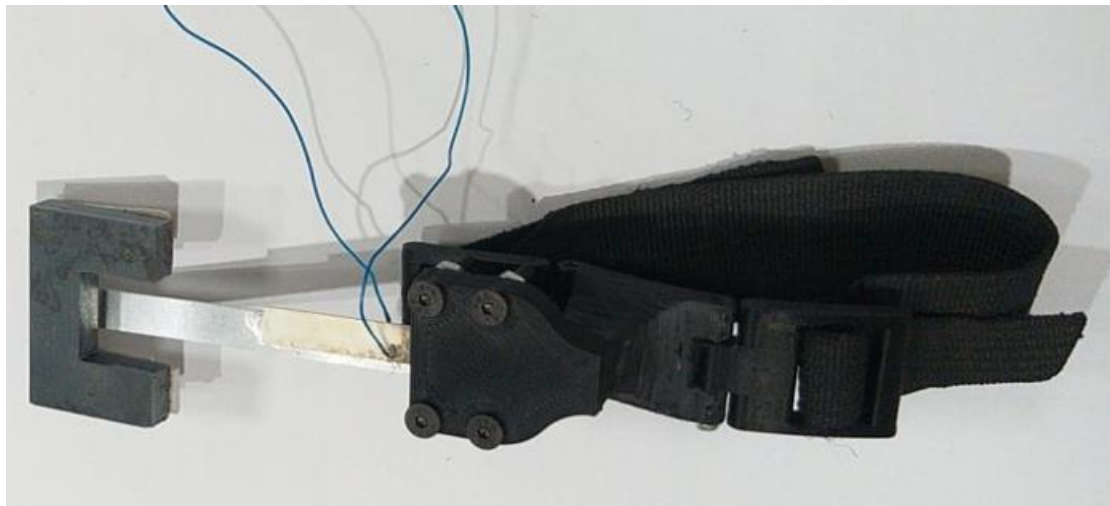


Figure 3.3.2 – Prototyped Energy Harvester assembled on the holding assembly



Figure 3.3.3 – Prototyped Energy Harvester held on the hand through strip

CHAPTER 4: FINITE ELEMENT METHOD

SolidWorks is used to model the piezoelectric energy harvester, which is then loaded into Ansys for finite element analysis. The resonant mode shapes and Eigen frequencies displayed in the results are utilized to tailor the system for the intended real-world application. The simulated model provided beam displacement of the proposed energy harvester corresponding to the resonant frequency and here we observed two mode shapes of the designed energy harvester, whose resonant frequency was around 8.0373 Hz. The first two harmonic modes of the system are shown in Figure 4.0.1 and Figure 4.0.2.

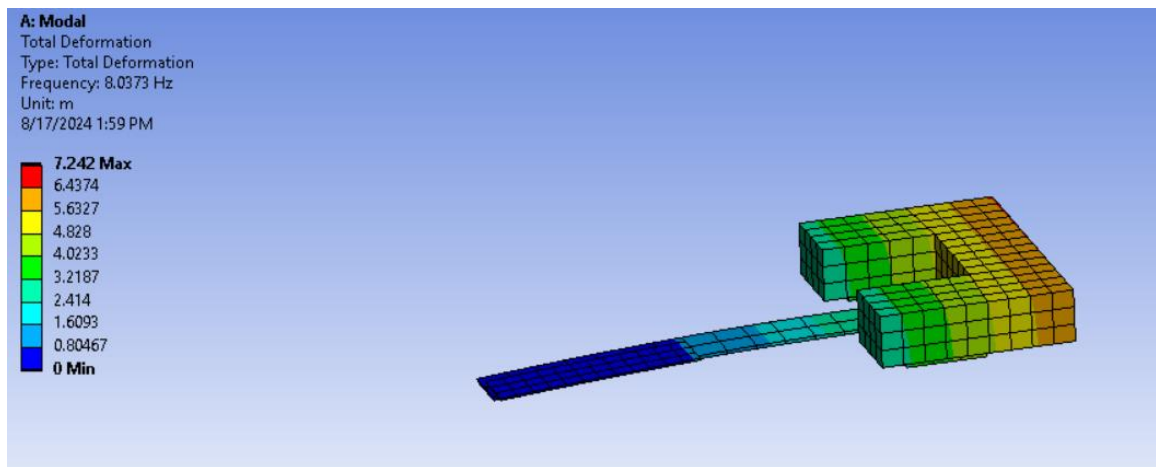


Figure 4.0.1 – Harmonic Frequency of the proposed model at first resonant frequency
(8.0373 Hz)

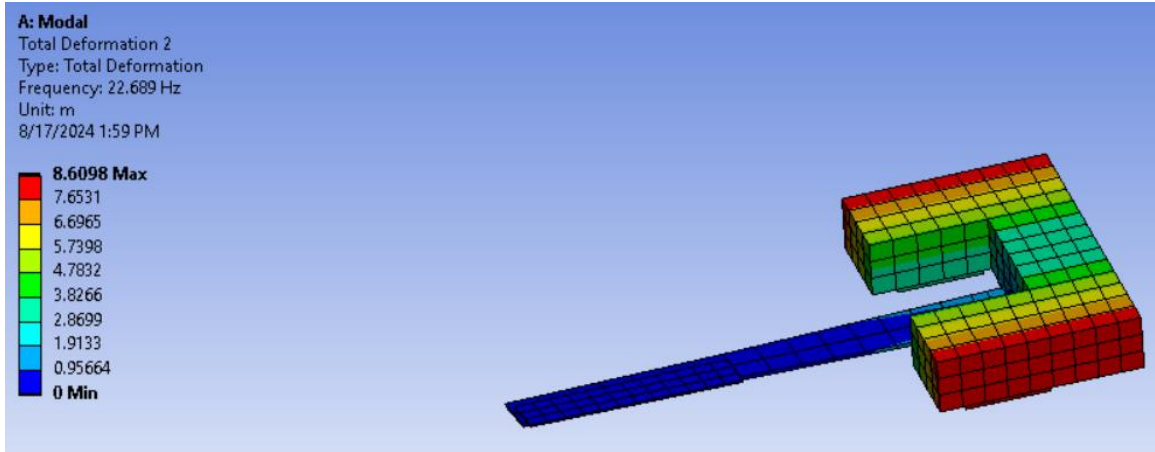


Figure 4.0.2 – Harmonic Frequency of the proposed model at second resonant frequency
(22.689 Hz)

Table 4.0.1: Material used and their properties

Element	Material	Properties
Body	Aluminum	Density – 2700 kgm-3 Young’s
		Modulus – 70 GPa Aluminum
		Piezoelectric Poisson Ratio – 0.33
Piezoelectric	PZT-5A	Density – 7800 kgm-3
		Loss Factor (Electrical Permittivity) – 0.02
		Coupling and Compliance Matrices Defined Individually
Proof Mass	Mild Steel	Density – 7850 kgm-3
		Young’s Modulus – 210 GPa
		Poisson Ratio – 0.3

CHAPTER 5: EXPERIMENTAL SETUP

The experimental setup for the test is shown in the following diagram. A mechanical shaker (Smart Shaker K2007E01) with a maximum force output of 31N and suitable for frequencies up to 9000Hz is used for the test. The shaker receives information from a function generator. This function generator (GW Instek AFG-2012) is connected to a power amplifier (Smart Amp 2100E21) to provide the required harmonic intensity. The ability of the instrument to generate a wide range of input frequencies allowed a comprehensive analysis of the collector response across the entire frequency spectrum. An MPU 6050 accelerometer is used to track the acceleration. A Hantek DSO5202P oscilloscope was used to test the output voltage of the system.



Figure 5.0.1 – Photograph of the Function Generator



Figure 5.0.2 – Photograph of the Vibration Exciter



Figure 5.0.3 – Photograph of the Power Amplifier



Figure 5.0.4 – Photograph of the Digital Oscilloscope

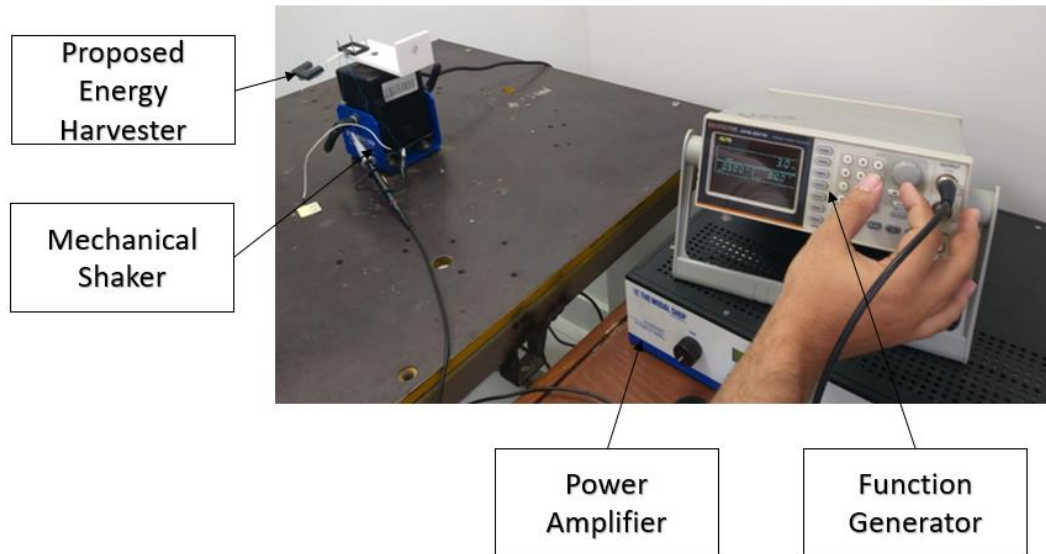


Figure 5.0.5 – Photograph of the Experimental setup with fabricated proposed Energy Harvester prototype

A complete overview of the experimental setup used to evaluate the proposed energy harvester is shown in Figure 5.0.1 to Fig. 5.0.5. The schematic connection diagram shown in Figure 5.0.1 provides a clear visual indication of how the different components of the test equipment are interconnected. High-resolution images of each part used in the experiments are shown in Figures 5.0.2 - 5.0.4. The final setup is shown in Figure 5.0.5, which includes a photograph of the complete experimental setup in which the energy harvester prototype was built. A mechanical shaker on which the proposed energy harvester was securely mounted. This shaker served to provide tuned sinusoidal stimuli to the combine that mimicked the vibrations found in a real environment. By adjusting the frequency and acceleration of these stimuli, the combined performance could be carefully tested in different configurations. A function generator was used to generate the various operating frequencies required for the experiments. To complement the function generator, a power amplifier was used to adjust the amplitude of the acceleration applied to the shaker.

The testing process involves sending a cyclic load waveform from a signal generator, through a power amplifier, and finally to the electrodynamic agitator. The output terminals of the energy harvester were immediately connected to a digital oscilloscope to measure and record the output response. This high-precision instrument allows for precise measurement and visualization of the electrical signals generated by the combine in response to the applied mechanical vibrations

5.1 Results and Discussion

To evaluate the performance of the proposed energy harvester at different frequencies, extensive tests were conducted using a specially designed experimental setup. As per the figures, the voltage output showed considerable peaks at certain frequencies. The system showed the best performance, producing an impressive 11.44V at 7.5Hz. To better understand the frequency response, tests were performed at closer frequencies. The coupling produced 8.12V, just below the ideal frequency of 7.4Hz. Similarly, the output reached 9.92V at 7.6Hz, just above the peak. The performance of the device rises sharply towards 7.5Hz and then drops off as the frequency moves away from this optimum point, with the data clearly showing a vertical performance curve. These results highlight how sensitive the combine is to frequency changes and how important precise tuning is to improving power production. The large change in voltage output over a small range of 0.2 Hz highlights how important frequency matching is in piezoelectric energy harvesting applications.

Fig. 5.1.1 shows the beam frequency response characteristics of the proposed piezoelectric energy harvester. The prototype displays a unique vibration mode that

generates a unique peak in the voltage output, which is consistent with the analytical expectations.

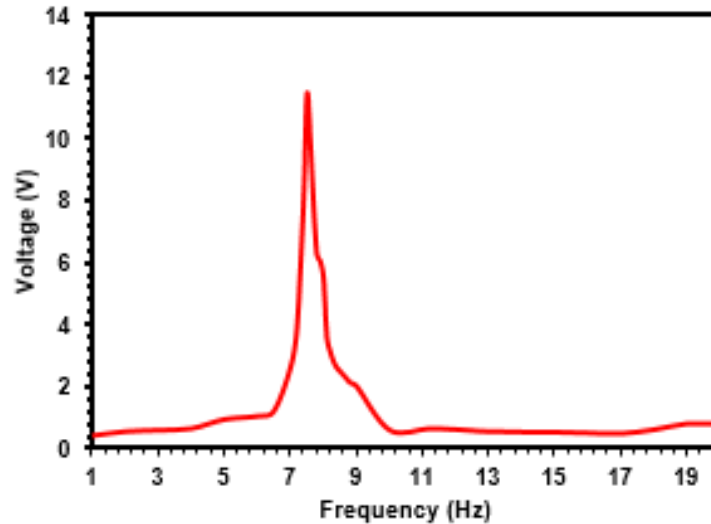


Figure 5.1.1 – Frequency response of the proposed energy harvester

A closer look at the voltage response curves reveals that the developed energy harvester reaches resonance at 7.5 Hz, and the finite element method (FEM) simulation results, which predicted the resonant frequency to be 8.073 Hz, closely matched the experimental results.

Several reasons, including manufacturing tolerances and small differences between modeled and actual material properties, could be attributed to the small difference between the simulated and observed frequencies. The prototype performed well in an open-circuit environment, achieving a maximum voltage of approximately 11.44 V at the resonant frequency.

The optimum energy conversion efficiency of the combine is represented by the maximum voltage generated when the mechanical vibration frequency matches the natural frequency of the device. The strong agreement between the simulation predictions and the experimental results confirms the validity of the FEM model and highlights the efficiency of the proposed design.

Furthermore, the considerable resonant voltage output of the energy harvester indicates its practical usability in environments with typical vibration rates of approximately 7.5 Hz.

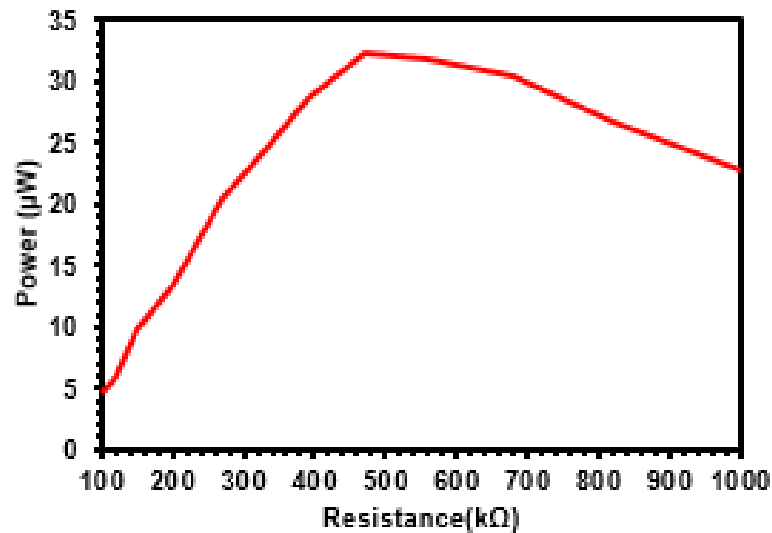


Figure 5.1.2 – Output power vs Load resistor of the piezoelectric beam of the proposed energy harvester at 7.4 Hz

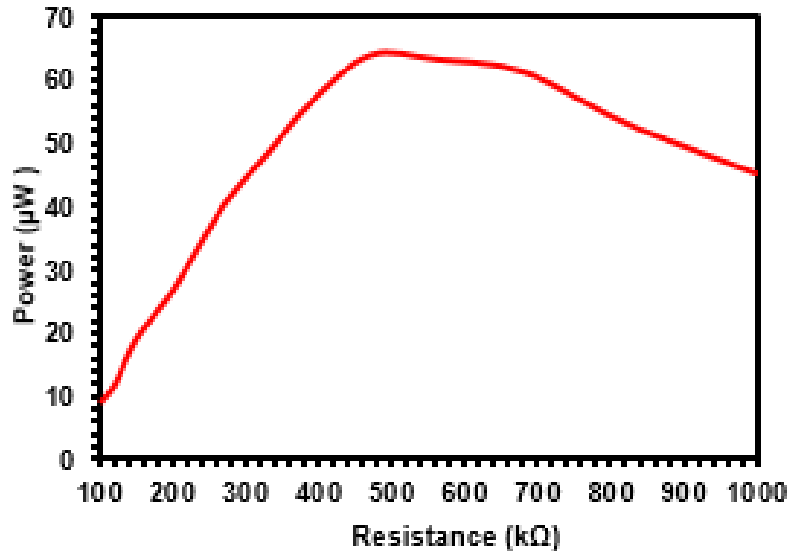


Figure 5.1.3 – Output power vs Load resistor of the piezoelectric beam of the proposed energy harvester at 7.5 Hz

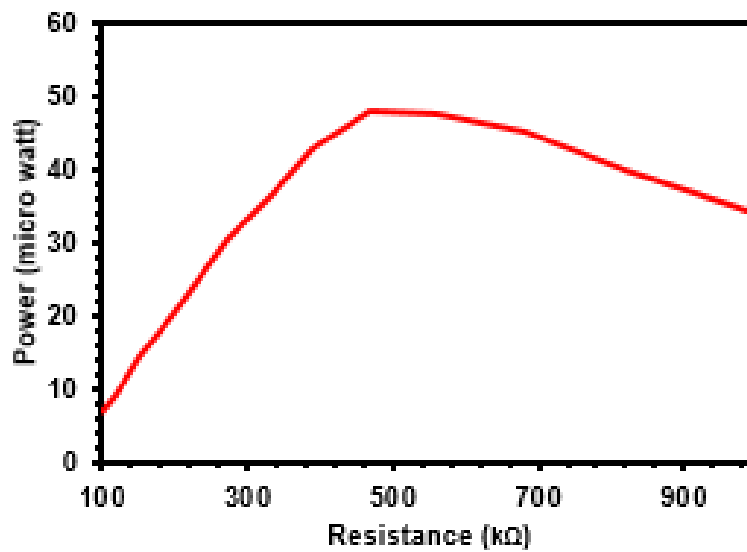


Figure 5.1.4 – Output power vs Load resistor of the piezoelectric beam of the proposed energy harvester at 7.6 Hz

Further tests were conducted focusing on the power output characteristics of the proposed energy harvesting device to evaluate its performance further. These studies were conducted on a single piezoelectric module beam at a given resonant frequency of 7.5Hz with a base acceleration of 0.2m/s^2 . The power and voltage output are measured with different load resistors. Fig. 5.1.2, Fig. 5.1.3, and Fig. 5.1.4 show the results. The graphs provide an overall overview of how the device's performance changes with different electrical loads.

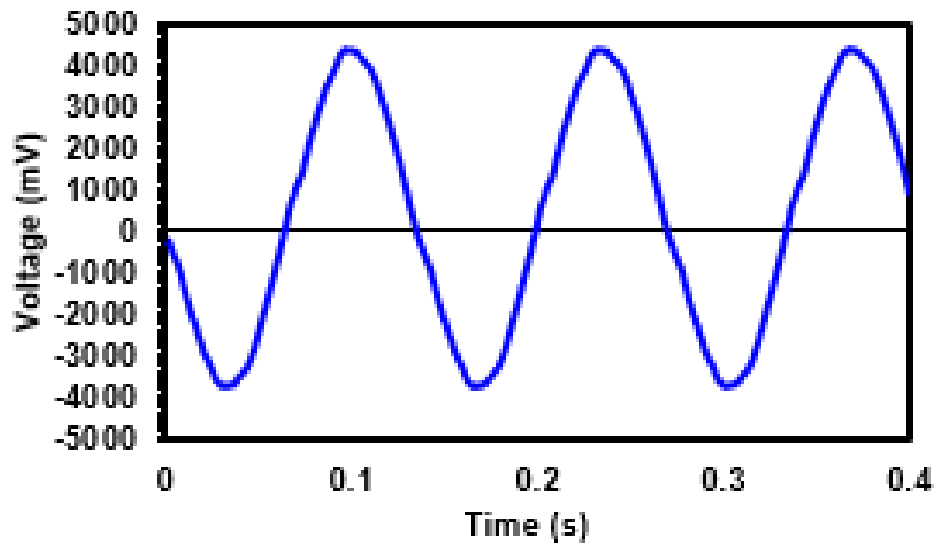


Figure 5.1.5 – Instantaneous voltage waveform generated by the single piezo element of the proposed energy harvester prototype at 7.4 Hz

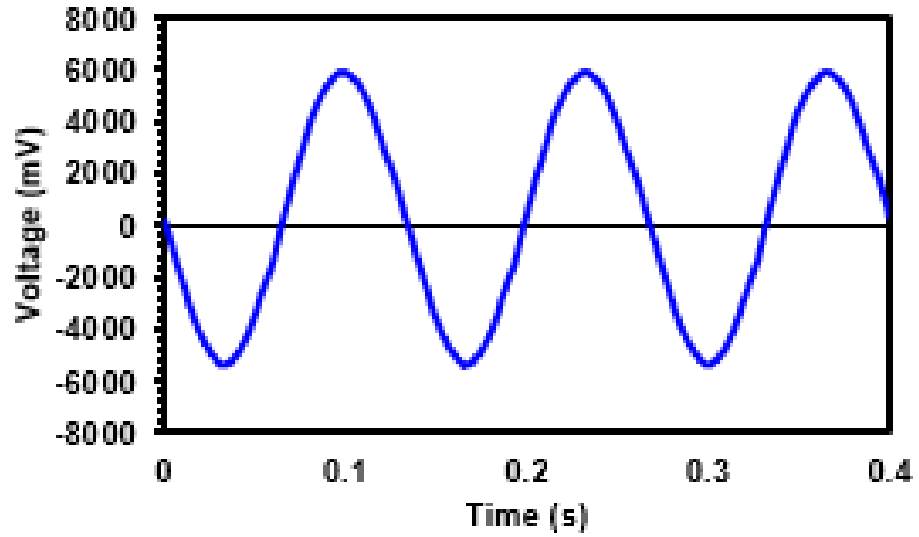


Figure 5.1.6 – Instantaneous voltage waveform generated by the single piezo element of the proposed energy harvester prototype at 7.5 Hz

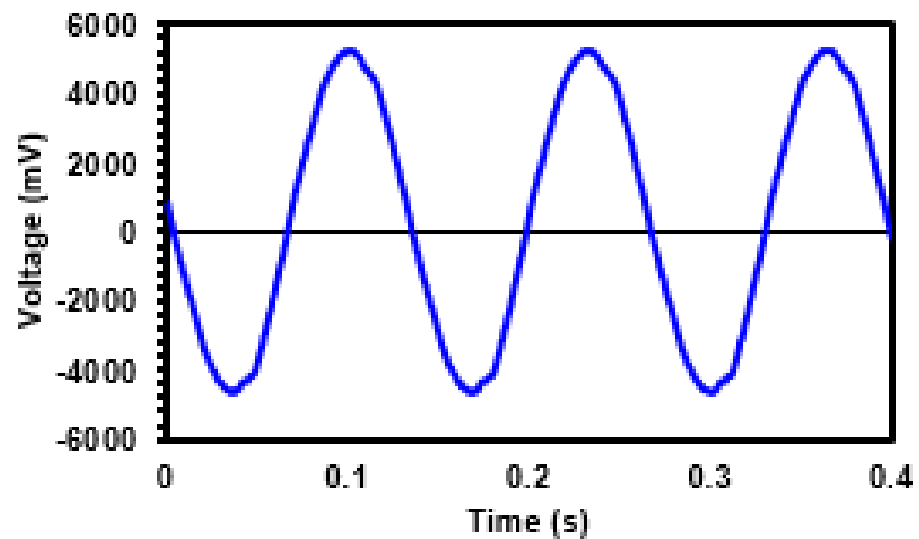


Figure 5.1.7 – Instantaneous voltage waveform generated by the single piezo element of the proposed energy harvester prototype at 7.6 Hz

Experiments show that the maximum output power is reached when the device is connected to a load resistance of 470 kilo-ohms. Operating at the resonant frequency, the energy harvester produced a maximum output power of approximately 63.89 micro-watts.

The voltage output of a single harvester prototype piezo element is shown in Fig. 5.1.15, Fig. 5.1.16, and Fig. 5.1.17. Three fundamental frequencies were used to record the waves; the resonant frequency is 7.5 Hz, and two adjacent frequencies are 7.4 Hz and 7.6 Hz, occurring at a cyclic acceleration of 0.2m/s^2 . The harvester operates at maximum efficiency at a resonant frequency of 7.5 Hz, producing a peak-to-peak voltage of 11.44 V.

CHAPTER 6: CONCLUSION

This study presents a novel design the SDOF wearable Energy Harvester as a tremor sensor that doctors can wear on their hands while performing surgery. We have done a FEM simulation of the proposed design for the resonant frequency that we got around 8.0373 Hz and approximate voltage. Upon experimenting, the resonant frequency of the system is achieved at 7.5 Hz and the maximum peak-to-peak voltage is 11.44 V in open circuit at the acceleration of 0.2m/s^2 . While experimenting with the resistor, the maximum power obtained is about 63.69 micro-watts with the resistor of 470 kilohms. This sensors have shown exceptional results in detecting the human hand's tremors they can be used by both doctors during surgery and the detection of the tremors in the patient's hand especially patients ill with Parkinson's disease, which can be further exploited in biomedical applications.

References

- [1] G. Lai, W. Liu, W. Yang, H. Zhong, Y. He, and Y. Zhang, "An Incremental Broad-Learning-System-Based Approach for Tremor Attenuation for Robot Tele-Operation," pp. 1–18, 2023.
- [2] Z. Liu, Q. Wu, Y. Zhang, Y. Wang, and C. L. P. Chen, "Adaptive fuzzy wavelet neural network filter for hand tremor cancelling in microsurgery," *Appl. Soft Comput.*, vol. 11, no. 8, pp. 5315–5329, 2011, doi: <https://doi.org/10.1016/j.asoc.2011.05.027>.
- [3] Z. Liu, C. Mao, J. Luo, Y. Zhang, and C. L. Philip Chen, "A three-domain fuzzy wavelet network filter using fuzzy PSO for robotic assisted minimally invasive surgery," *Knowledge-Based Syst.*, vol. 66, pp. 13–27, 2014, doi: <https://doi.org/10.1016/j.knosys.2014.03.025>.
- [4] X. Li, S. Guo, P. Shi, X. Jin, M. Kawanishi, and K. Suzuki, "A Bimodal Detection-Based Tremor Suppression System for Vascular Interventional," *IEEE Trans. Instrum. Meas.*, vol. 71, pp. 1–12, 2022, doi: [10.1109/TIM.2022.3216367](https://doi.org/10.1109/TIM.2022.3216367).
- [5] M. Roizenblatt, A. Ebrahimi, I. Iordachita, and P. L. Gehlbach, "Robotic Systems in Ophthalmologic Surgery," pp. 161–174, 2023.
- [6] M. Yousef, M. Hafizh, S. Sassi, and G. Adeli, "Development of a Wearable Wireless Sensing Device for Characterization of Hand Tremors Through Vibration Frequency Analysis," *J. Vib. Eng. Technol.*, vol. 11, no. 7, pp. 3109–3120, 2023, doi: [10.1007/s42417-022-00734-2](https://doi.org/10.1007/s42417-022-00734-2).
- [7] M. Roizenblatt, A. T. Grupenmacher, R. Belfort Junior, M. Maia, and P. L. Gehlbach, "Robot-Assisted tremor control for performance enhancement of retinal microsurgeons," *Br. J. Ophthalmol.*, vol. 103, no. 8, pp. 1195–1200, 2019, doi: [10.1136/bjophthalmol-2018-313318](https://doi.org/10.1136/bjophthalmol-2018-313318).
- [8] R. J. Elble, "What is essential tremor? Topical collection on movement disorders," *Curr. Neurol. Neurosci. Rep.*, vol. 13, no. 6, 2013, doi: [10.1007/s11910-013-0353-4](https://doi.org/10.1007/s11910-013-0353-4).
- [9] S. Tatinati, K. C. Veluvolu, and W. T. Ang, "Multistep Prediction of Physiological Tremor Based on Machine Learning for Robotics Assisted Microsurgery," *IEEE Trans. Cybern.*, vol. 45, no. 2, pp. 328–339, 2015, doi: [10.1109/TCYB.2014.2381495](https://doi.org/10.1109/TCYB.2014.2381495).
- [10] M. Using and I. Sensors, "Drift-Free Position Estimation of Periodic or Quasi-Periodic Motion Using Inertial Sensors," pp. 5931–5951, 2011, doi: [10.3390/s110605931](https://doi.org/10.3390/s110605931).
- [11] R. Torah, M. Tudor, T. O. Donnell, and S. Roy, "Self-powered autonomous wireless sensor node using vibration energy harvesting," 2008, doi: [10.1088/0957-](https://doi.org/10.1088/0957-)

0233/19/12/125202.

- [12] A. Cadei, A. Dionisi, E. Sardini, and M. Serpelloni, “Kinetic and thermal energy harvesters for implantable medical devices and biomedical autonomous sensors,” 2014, doi: 10.1088/0957-0233/25/1/012003.
- [13] S. Materials, “A review of the recent research on vibration energy harvesting via bistable systems,” 2013, doi: 10.1088/0964-1726/22/2/023001.
- [14] M. A. Halim, H. Cho, and J. Y. Park, “Design and experiment of a human-limb driven, frequency up-converted electromagnetic energy harvester,” *Energy Convers. Manag.*, vol. 106, pp. 393–404, 2015, doi: <https://doi.org/10.1016/j.enconman.2015.09.065>.
- [15] N. G. Stephen, “On energy harvesting from ambient vibration,” *J. Sound Vib.*, vol. 293, no. 1, pp. 409–425, 2006, doi: <https://doi.org/10.1016/j.jsv.2005.10.003>.
- [16] M. A. Halim and J. Y. Park, “Theoretical modeling and analysis of mechanical impact driven and frequency up-converted piezoelectric energy harvester for low-frequency and wide-bandwidth operation,” *Sensors Actuators A Phys.*, vol. 208, pp. 56–65, 2014, doi: <https://doi.org/10.1016/j.sna.2013.12.033>.
- [17] N. Jackson and A. Mathewson, “A review of piezoelectric polymers as functional materials for electromechanical transducers”, doi: 10.1088/0964-1726/23/3/033001.
- [18] R. M. Toyabur, M. Salauddin, and J. Y. Park, “Design and experiment of piezoelectric multimodal energy harvester for low frequency vibration,” no. xxxx, 2017.
- [19] J. M. Ramírez, C. D. Gatti, S. P. Machado, and M. Febbo, “A multi-modal energy harvesting device for low-frequency vibrations,” vol. 22, pp. 1–7, 2018, doi: 10.1016/j.eml.2018.04.003.
- [20] J.-X. Wang, J.-C. Li, W.-B. Su, X. Zhao, and C.-M. Wang, “A multi-folded-beam piezoelectric energy harvester for wideband energy harvesting under ultra-low harmonic acceleration,” *Energy Reports*, vol. 8, pp. 6521–6529, 2022, doi: <https://doi.org/10.1016/j.egy.2022.04.077>.
- [21] D. F. Berdy *et al.*, “Low-Frequency Meandering Piezoelectric Vibration Energy Harvester,” *IEEE Trans. Ultrason. Ferroelectr. Freq. Control*, vol. 59, no. 5, pp. 846–858, 2012, doi: 10.1109/TUFFC.2012.2269.
- [22] R. Chen, L. Ren, H. Xia, X. Yuan, and X. Liu, “Energy harvesting performance of a dandelion-like multi-directional piezoelectric vibration energy harvester,” *Sensors Actuators A Phys.*, vol. 230, pp. 1–8, 2015, doi: <https://doi.org/10.1016/j.sna.2015.03.038>.
- [23] X. Bai, Y. Wen, P. Li, J. Yang, X. Peng, and X. Yue, “Sensors and Actuators A : Physical Multi-modal vibration energy harvesting utilizing spiral cantilever with magnetic coupling,” vol. 209, pp. 78–86, 2014.

- [24] C. Shi, F. Li, and J. Zhao, “energy harvester with low resonant frequency,” 2020, doi: 10.1063/5.0002844.
- [25] B. Andò, S. Baglio, A. R. Bulsara, and V. Marletta, “A bistable buckled beam based approach for vibrational energy harvesting,” *Sensors Actuators A Phys.*, vol. 211, pp. 153–161, 2014, doi: <https://doi.org/10.1016/j.sna.2013.12.027>.
- [26] W. Jiang, L. Wang, X. Wang, L. Zhao, and X. Fang, “Comparison of L-Shaped and U-Shaped Beams in Bidirectional Piezoelectric Vibration Energy Harvesting,” pp. 1–9, 2022.
- [27] N. Zhao *et al.*, “Three-dimensional piezoelectric vibration energy harvester using spiral-shaped beam with triple operating frequencies,” 2016, doi: 10.1063/1.4940417.
- [28] Y. Wu, J. Qiu, S. Zhou, H. Ji, Y. Chen, and S. Li, “A piezoelectric spring pendulum oscillator used for multi-directional and ultra-low frequency vibration energy harvesting,” *Appl. Energy*, vol. 231, pp. 600–614, 2018, doi: <https://doi.org/10.1016/j.apenergy.2018.09.082>.
- [29] C. Xia, D. F. Wang, T. Ono, T. Itoh, and M. Esashi, “Internal resonance in coupled oscillators – Part II: A synchronous sensing scheme for both mass perturbation and driving force with duffing nonlinearity,” *Mech. Syst. Signal Process.*, vol. 160, p. 107887, 2021, doi: <https://doi.org/10.1016/j.ymsp.2021.107887>.
- [30] Z. Yuan, W. Liu, S. Zhang, Q. Zhu, and G. Hu, “Bandwidth broadening through stiffness merging using the nonlinear cantilever generator,” *Mech. Syst. Signal Process.*, vol. 132, pp. 1–17, 2019, doi: <https://doi.org/10.1016/j.ymsp.2019.06.014>.
- [31] S. Ushiki and A. Masuda, “Toward self-powered nonlinear wideband vibration energy harvesting with high-energy response stabilization Toward self-powered nonlinear wideband vibration energy harvesting with high-energy response stabilization,” 2019, doi: 10.1088/1742-6596/1407/1/012011.
- [32] D. S. Bath, “Low-Frequency Piezoelectric Energy Harvester with Novel 3D Folded Zigzag Design and High Power Density,” 2018.
- [33] D. Han and K. Seok, “Piezoelectric energy harvester using mechanical frequency up conversion for operation at low - level accelerations and low - frequency vibration,” *Microsyst. Technol.*, vol. 21, no. 8, pp. 1669–1676, 2015, doi: 10.1007/s00542-014-2261-1.
- [34] R. Masana and M. F. Daqaq, “Response of duffing-type harvesters to band-limited noise,” *J. Sound Vib.*, vol. 332, no. 25, pp. 6755–6767, 2013, doi: <https://doi.org/10.1016/j.jsv.2013.07.022>.
- [35] “A nonlinear piezoelectric energy harvester with magnetic oscillator,” 2012, doi: 10.1063/1.4748794.

- [36] C. Kiong, "Improving functionality of vibration energy harvesters using magnets," pp. 0–44, 2012.
- [37] M. R. Sarker, S. Julai, M. F. M. Sabri, S. M. Said, M. M. Islam, and M. Tahir, "Review of piezoelectric energy harvesting system and application of optimization techniques to enhance the performance of the harvesting system," *Sensors Actuators A Phys.*, vol. 300, p. 111634, 2019, doi: <https://doi.org/10.1016/j.sna.2019.111634>.
- [38] A. Nisanth, "Design and optimization of MEMS piezoelectric energy harvester for low frequency applications," *Microsyst. Technol.*, vol. 27, no. 1, pp. 251–261, 2021, doi: [10.1007/s00542-020-04944-0](https://doi.org/10.1007/s00542-020-04944-0).